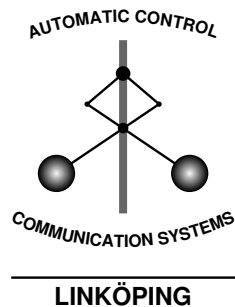


Detection and Estimation of Nonlinear Distortions in Industrial Robots

Erik Wernholt, Svante Gunnarsson

Division of Automatic Control
Department of Electrical Engineering
Linköpings universitet, SE-581 83 Linköping, Sweden
WWW: <http://www.control.isy.liu.se>
E-mail: erikw@isy.liu.se, svante@isy.liu.se

29th August 2006



Report no.: LiTH-ISK-R-2740

Accepted for publication in IMTC 2006, Sorrento, Italy

Technical reports from the Control & Communication group in Linköping are available at <http://www.control.isy.liu.se/publications>.

Abstract

System identification in robotics often involves the estimation of linear models characterizing the behavior in certain operating points. In this paper, a method for the detection and estimation of nonlinear distortions in an estimated frequency response function (FRF) has successfully been applied to experimental data from an industrial robot. The results show that nonlinear distortions are indeed present and cause larger variability in the FRF than the measurement noise contributions.

Keywords: Frequency response functions, multivariable systems, nonlinear distortions, non-parametric identification, industrial robots

Detection and Estimation of Nonlinear Distortions in Industrial Robots

Erik Wernholt and Svante Gunnarsson

Department of Electrical Engineering, Linköping University,
SE-581 83 Linköping, Sweden.
E-mail: {erikw,svante}@isy.liu.se.

Abstract – System identification in robotics often involves the estimation of linear models characterizing the behavior in certain operating points. In this paper, a method for the detection and estimation of nonlinear distortions in an estimated frequency response function (FRF) has successfully been applied to experimental data from an industrial robot. The results show that nonlinear distortions are indeed present and cause larger variability in the FRF than the measurement noise contributions.

Keywords – Frequency response functions, multivariable systems, nonlinear distortions, non-parametric identification, industrial robots

I. INTRODUCTION

Industrial robots pose a challenging problem for system identification methods. Usually a robot has six joints, with coupled dynamics, giving a truly multivariable system. The dynamics are nonlinear, both with respect to the operating point and other nonlinearities such as friction, torque and resolver ripple, backlash, hysteresis, and nonlinear stiffness in the transmission. The robot arm and transmission are more or less elastic and, in addition, the data collection must usually be carried out in closed loop.

The identification of such a complex system is a huge task, both in finding suitable model structures and efficient identification procedures, and is still a research topic. Under certain simplifying assumptions, a subset of the parameters can be identified. Neglecting elastic effects, a nonlinear model of the rigid body dynamics can be estimated using least squares techniques. This is a much studied problem in the literature (see, for example, [1]). Taking elastic effects into account makes the identification problem more involved, since now typically only a subset of the state variables are measured and one can therefore not use linear regression. A common remedy then is to study the dynamic behavior around certain operating points (see, for example, [2], [3], [4], [5]). Often this results in a linear model for each working point.

One application area for linear models is control design, where a global controller is achieved through gain scheduling. The linear models could also be used for the tuning of elastic parameters (typically springs and dampers) in a global nonlinear elastic model. For both of these application areas, it is important that the estimated linear models are accurate, or at

least are delivered with some estimated uncertainty regions. In the presence of nonlinearities, these uncertainty regions tend to be underestimated. It is therefore of great importance to use an identification procedure that can detect the presence of nonlinearities and in addition quantify how the estimated models are affected.

In this work, a method first introduced in [6], [7] will be evaluated for the robot application using experimental data. The method makes it possible to detect the presence of nonlinearities and quantify how much they affect the nonparametric estimate of the frequency response function (FRF). The method was developed for open loop SISO measurements, but will here be applied to both closed loop SISO and MIMO measurements. Applying their method to experimental data from a MIMO system is, to our knowledge, a new result.

II. MEASUREMENT SETUP

The data used for identification are collected from an experimental industrial robot system, similar to the ABB IRB6600 robot in Figure 1. Each axis of the robot arm is actuated by an electric motor via a transmission and the movements are controlled by a computer system. The first three axes will be considered in this work, giving a multivariable system with three inputs (commanded motor torques) and three outputs (motor velocities). For this kind of application it is necessary to use feedback control while data are collected, both for safety reasons and in order to keep the robot around its operation point.

Consider therefore the setting in Figure 2, where F is the controller and G is the robot subject for identification. The controller takes as input the difference between the reference signal r and the measured and sampled output y , and u is the commanded input. Due to disturbances v_u and v_y , the input will be $u_p = u + v_u$ and the measured output $y = y_p + v_y$, i.e., the sum of the true output y_p and the output disturbance v_y .

An experimental control system is used, which makes it possible to use off-line computed reference signals for each motor controller. The excitation signals are applied as reference signals for the motor velocities. The experimental controller can approximately be seen as a diagonal PI-controller.

For this particular industrial robot, the motor position φ is measured using Tracking Resolver-to-Digital Converters [8].

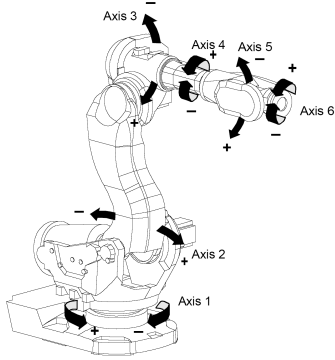


Fig. 1. The ABB IRB6600 robot.

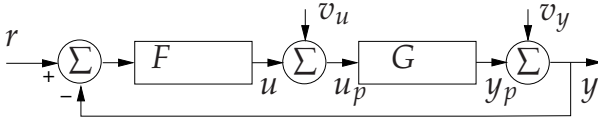


Fig. 2. Closed loop measurement setup.

The measured position is then filtered and differentiated to obtain an estimate of the motor velocity, which is here considered as the output signal. It is shown in [8] that the position measurement error v_φ , due to non-ideal resolver characteristics, can be described as a sum of sinusoids like in

$$v_\varphi(t) = \sum_{n \in \mathbb{N}_c} c_n \sin(n\varphi(t) + \phi_{c,n}), \quad (1)$$

with amplitudes c_n , phases $\phi_{c,n}$, and \mathbb{N}_c a set of integers.

AC permanent magnet motors are used as actuators, which will give rise to torque ripple. The ripple can be modeled as sums of sinusoids similar to (1) but with additional terms proportional to the motor current, see [9] for details.

As transmission, harmonic drives are very popular today due to their low backlash, compact size, and high torque transmission. Using harmonic drives will however introduce nonlinear stiffness, friction, and kinematic errors. This shows up as hysteresis curves when torque is plotted against angular displacements [10].

III. ESTIMATION PROCEDURE

The aim of the estimation procedure from [6], [7] is to find a non-parametric estimate of the frequency response function (FRF) relating the DFTs of the input and output signals, like

$$Y(\omega_k) = G(\omega_k)U(\omega_k) \quad (2)$$

where $G(\omega_k)$ is a short notation for $G(e^{i\omega_k T_s})$. The FRF will be measured using random phase multisines as excitation signals, which are defined as

$$r(t) = \sum_{k=1}^{N/2} A_k \sin(\omega_k t + \phi_k), \quad (3)$$

with amplitudes A_k , phases ϕ_k , and frequencies $\omega_k = \frac{2\pi k}{N} f_s$. The phases ϕ_k are randomly chosen such that $E\{e^{j\phi_k}\} = 0$, for example uniformly distributed in $[0, 2\pi)$. For sampled data, f_s is the sample frequency and each period of data then has N samples and a period time $T_0 = \frac{N}{f_s}$.

Using random phase multisines as input signal in an open loop setting, with N sufficiently large, the FRF of a wide class of nonlinear systems can be written as

$$G(\omega_k) = G_R(\omega_k) + G_S(\omega_k) + N_G(\omega_k) \quad (4)$$

with $G_R(\omega_k)$ the best linear approximation to the nonlinear system, $G_S(\omega_k)$ a zero mean stochastic nonlinear contribution, and $N_G(\omega_k)$ the measurement noise (see [11] for details). For different realizations of the excitation signal, the stochastic nonlinear contribution, $G_S(\omega_k)$, acts as circular complex noise when N is sufficiently large. Therefore $G_S(\omega_k)$ cannot be distinguished from the measurement noise. Still, once the excitation signal is fixed, $G_S(\omega_k)$ is a deterministic component. The linear approximation, $G_R(\omega_k)$, is independent of the random phase of the random multisine excitation.

For closed loop data, the properties of the estimate are much harder to analyze, mainly since the input signal no longer is distributed as desired. The input signal will be correlated with the measurement noise which, even in a linear setting, will give biased FRF estimates (see, for example, [12], [13]). What is worse, the input signal will also be affected by the nonlinearities through the feedback and will therefore not be Gaussian distributed. The estimation method can still be applied to closed loop data, but the resulting estimates must be further analyzed to be able to draw any detailed conclusions.

To be able to distinguish between the measurement noise and the stochastic nonlinear contributions, two different measurement strategies were proposed in [6], [7]. The first strategy uses a single experiment with $P \geq 6$ periods of the steady state response. The excitation signal is a random phase multisine signal containing only odd frequencies, where certain odd frequencies are eliminated as well. The nonlinear stochastic contributions are then found by extrapolation, see [6], [7] for details. Here, their second strategy will be used, which requires $M \geq 6$ different experiments with $P \geq 2$ periods in each experiment¹. This is more time consuming and will not give a classification in odd and even degree nonlinear distortions. Still, no approximation (extrapolation) is used and the strategy can easily be extended to the multivariable case.

To simplify the notation, the estimation procedure will now be described for the SISO case. From the measurements, $M \times P$ FRFs, $\hat{G}^{[m,p]}(\omega_k)$, can be calculated like

$$\hat{G}^{[m,p]}(\omega_k) = \frac{Y^{[m,p]}(\omega_k)}{U^{[m,p]}(\omega_k)} \quad (5)$$

where $U^{[m,p]}(\omega_k)$ and $Y^{[m,p]}(\omega_k)$ are the DFTs of the input and output signals from period p in experiment m .

¹ Needed if the FRF estimate is used in a parametric modeling step to preserve the properties of the ML estimator [11].

For each experiment, one can calculate the average FRF $\hat{G}^{[m]}$ and its sample variance $\hat{\sigma}_{\hat{G}^{[m]}}^2$

$$\hat{G}^{[m]} = \frac{1}{P} \sum_{p=1}^P \hat{G}^{[m,p]} \quad (6)$$

$$\hat{\sigma}_{\hat{G}^{[m]}}^2 = \sum_{p=1}^P \frac{|\hat{G}^{[m,p]} - \hat{G}^{[m]}|^2}{P(P-1)} \quad (7)$$

The final FRF \hat{G} and its sample variance are obtained by averaging over the M experiments like

$$\hat{G} = \frac{1}{M} \sum_{m=1}^M \hat{G}^{[m]} \quad (8)$$

$$\hat{\sigma}_{\hat{G}}^2 = \sum_{m=1}^M \frac{|\hat{G}^{[m]} - \hat{G}|^2}{M(M-1)} \quad (9)$$

From (4), (7) and (9) it follows that

$$\mathbb{E} \{ \hat{\sigma}_{\hat{G}^{[m]}}^2 \} = \frac{\sigma_{N_G}^2}{P} \quad (10)$$

$$\mathbb{E} \{ \hat{\sigma}_{\hat{G}}^2 \} = \frac{\sigma_{G_S}^2 + \frac{\sigma_{N_G}^2}{P}}{M} \quad (11)$$

Hence, for a linear system ($G_S = 0$), $\hat{\sigma}_{\hat{G}}^2$ should originate from the stochastic noise source and therefore be equal to

$$\hat{\sigma}_{\hat{G}_n}^2 = \frac{1}{M^2} \sum_{m=1}^M \hat{\sigma}_{\hat{G}^{[m]}}^2 \quad (12)$$

If $\hat{\sigma}_{\hat{G}}^2$ is larger than $\hat{\sigma}_{\hat{G}_n}^2$, this indicate a nonlinear behavior and

$$\hat{\sigma}_{G_S}^2 = \max \left(M \left(\hat{\sigma}_{\hat{G}}^2 - \hat{\sigma}_{\hat{G}_n}^2 \right), 0 \right) \quad (13)$$

is a variance estimate for the stochastic nonlinear contribution.

For the MIMO case (n_y outputs, n_u inputs), the input vector is not invertible and it is therefore impossible to calculate an estimate like in (5) directly from data. To handle this, $M \cdot n_u$ experiments are carried out. For each block m of n_u experiments, the sampled data are collected into matrices, $\mathbf{U}^{[m,p]}(\omega_k) \in \mathbb{C}^{n_u \times n_u}$ and $\mathbf{Y}^{[m,p]}(\omega_k) \in \mathbb{C}^{n_y \times n_u}$ (bold face in the sequel) where each column corresponds to one experiment. The relation between the input and output can then be written as

$$\mathbf{Y}^{[m,p]}(\omega_k) = G(\omega_k) \mathbf{U}^{[m,p]}(\omega_k) \quad (14)$$

If $\mathbf{U}(\omega_k)$ has full rank, an estimate of $G(\omega_k)$ can be formed as

$$\hat{G}(\omega_k) = \mathbf{Y}^{[m,p]}(\omega_k) (\mathbf{U}^{[m,p]}(\omega_k))^{-1}(\omega_k) \quad (15)$$

To obtain variance expressions for the MIMO case, a similar procedure can be applied like in (6) – (13), but now taken element-wise.

As excitation signals, *orthogonal random phase multisines* [14] will be used. For each block of n_u experiments, the reference signal is calculated as

$$\mathbf{R}(\omega_k) = \begin{pmatrix} w_{11}R_1(\omega_k) & w_{12}R_1(\omega_k) & \dots & w_{1n_u}R_1(\omega_k) \\ w_{21}R_2(\omega_k) & w_{22}R_2(\omega_k) & \dots & w_{2n_u}R_2(\omega_k) \\ \dots & \dots & \dots & \dots \\ w_{n_u1}R_{n_u}(\omega_k) & w_{n_u2}R_{n_u}(\omega_k) & \dots & w_{n_un_u}R_{n_u}(\omega_k) \end{pmatrix}$$

where w_{kn} are elements of an arbitrary, deterministic, orthogonal matrix W . For each of the M blocks, a vector $R(\omega_k) = [R_1(\omega_k) R_2(\omega_k) \dots R_{n_u}(\omega_k)]^T$ of random phase multisines is generated for the first experiment. In the following $n_u - 1$ experiments, the elements of the vector are shifted orthogonally. Here, the elements of W are chosen as $w_{kn} = e^{\frac{2\pi i}{n_u}(k-1)(n-1)}$.

IV. RESULTS

To illustrate the estimation procedure, both SISO and MIMO experiments have been carried out. For the SISO case, only axis 1 of the industrial robot is excited. The SISO measurements are easier to analyze and give insights that can be used when trying to analyze the MIMO experiments. As excitation, an odd random phase multisine signal ($A_{2k} = 0$) will be used as motor velocity reference with period time $T_0 = 10$ s. A flat amplitude spectrum is used in the frequency interval 1–40 Hz, giving 195 excited frequencies. The commanded input u and measured output y are both sampled at $f_s = 2$ kHz.

Since nonlinear effects are studied, the results will vary with the excitation signal, such as its shape and amplitude. This is, for example, the case when having a nonlinear spring stiffness in the transmission. Typically, the spring gets stiffer for larger amplitudes. Different signal amplitudes will be studied for the MIMO case. To reduce the effect of static friction, it is common to use an excitation signal which avoids zero velocity crossings as much as possible. Therefore some experiments are carried out where the multisine signal is superimposed on a filtered square wave with period $T_0 = 10$ s and cut-off frequency 1 Hz.

A. SISO measurements

Two different data sets (with and without the filtered square wave) are collected with amplitudes according to Table I. For each data set, $M = 6$ experiments are performed and $P = 2$ periods of the steady state response are collected.

The estimation procedure according to (6) – (13) is then applied to the two different data sets. The estimated FRF, \hat{G} , can be seen in Figures 3 and 4 together with one standard deviation of the total sample variance $\hat{\sigma}_{\hat{G}}$ and the noise sample variance $\hat{\sigma}_{\hat{G}_n}$. As can be seen, nonlinear distortions are indeed present and cause larger variability in the FRF than the measurement noise contributions. Using the filtered square wave also gives more pronounced resonances since the influence of static friction is reduced.

Since the nonlinear distortions give larger variability than the measurement noise, averaging over different experiments

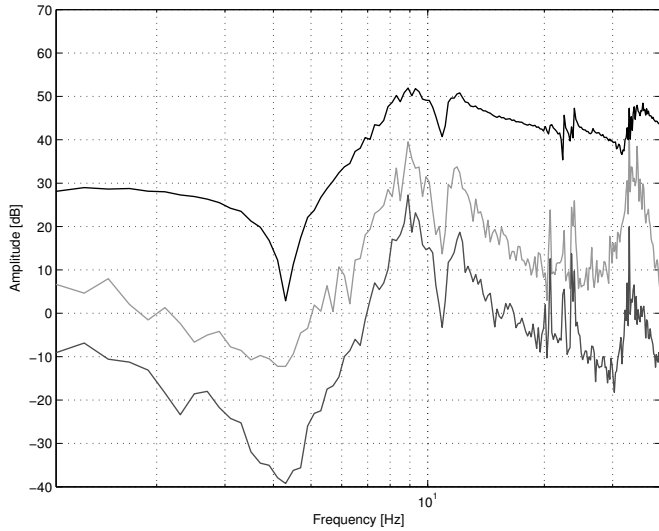


Fig. 3. Estimated FRF \hat{G} (black line) using data set 1. Grey line: standard deviation of the total sample variance $\hat{\sigma}_{\hat{G}}$. Dark grey line: standard deviation of the noise sample variance $\hat{\sigma}_{\hat{G}_n}$.

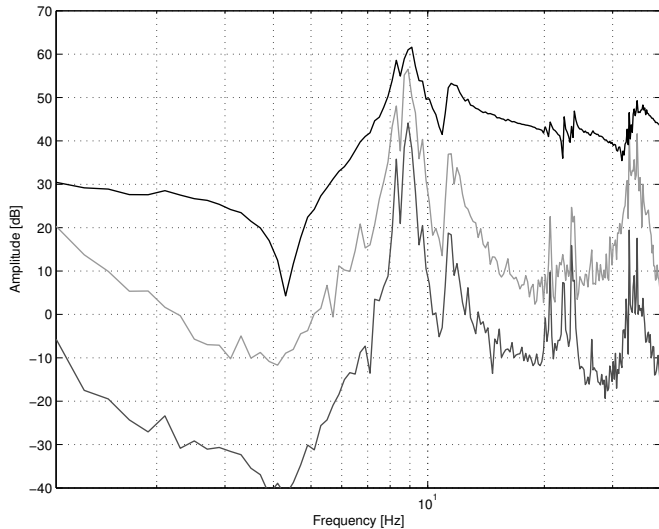


Fig. 4. Estimated FRF \hat{G} (black line) using data set 2. Grey line: standard deviation of the total sample variance $\hat{\sigma}_{\hat{G}}$. Dark grey line: standard deviation of the noise sample variance $\hat{\sigma}_{\hat{G}_n}$.

TABLE I
SIGNAL AMPLITUDES FOR THE SISO DATA SETS.

Data set	Multisine	Square wave
1	16	-
2	16	20

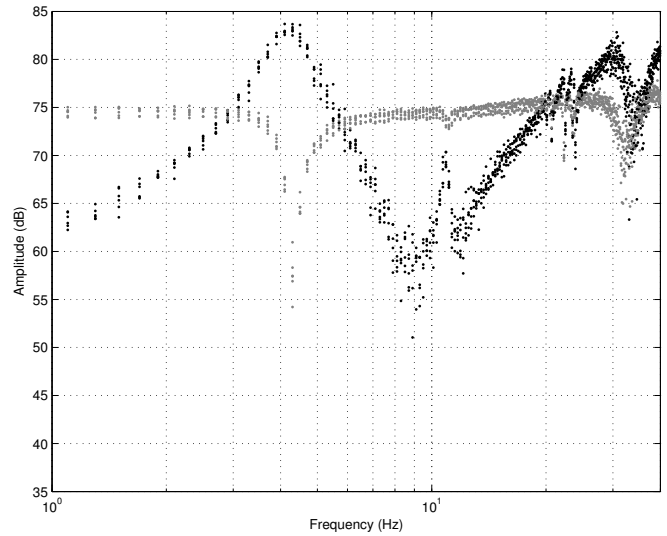


Fig. 5. Input spectrum (black) and output spectrum (grey) for the five experiments of data set 1.

TABLE II
SIGNAL AMPLITUDES FOR THE MIMO DATA SETS.

Data set	Multisine	Square wave
3	5	6
4	10	12
5	10	-

is important in order to get a more accurate FRF estimate. Averaging over several periods will not be as effective since that only reduce the measurement noise contributions.

A somewhat puzzling result is that the variance in the estimate is increased around the resonance frequency at 9 Hz when using the filtered square wave. In Figures 5 and 6 the input and output spectra are plotted for the two different data sets. By comparing the input spectra for the two cases it can be seen that without the filtered square wave the input power around the resonance frequency is larger. This is reasonable since the static friction acts as an increased damping, which in turn requires a larger input signal in order to follow the reference signal. Assuming similar noise levels, the filtered square wave will therefore give a lower input signal-to-noise ratio (SNR). A too low input SNR is therefore a probable explanation for the large variance around the resonance frequency. According to [6], the input SNR should be at least 6 dB to be able to ignore the relative bias in the FRF estimate. See also [11] for further details.

B. MIMO measurements

For the MIMO case, three different data sets are collected with amplitudes according to Table II. For each data set, $M = 9$ blocks of experiments are performed and $P = 2$ periods of the steady state response are collected.

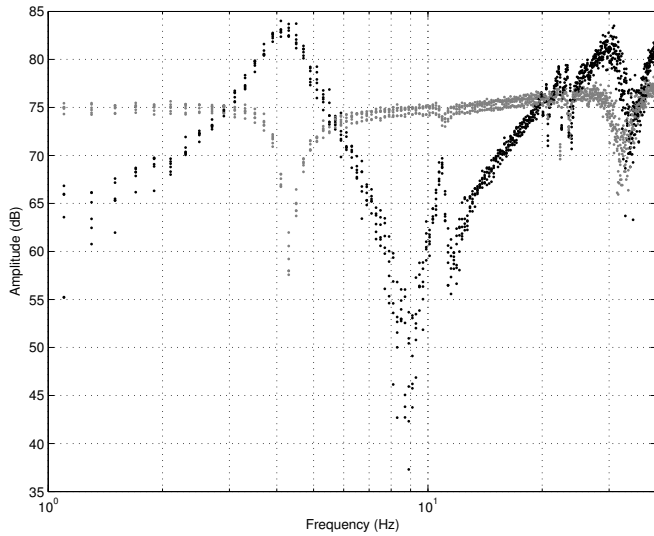


Fig. 6. Input spectrum (black) and output spectrum (grey) for the five experiments of data set 2.

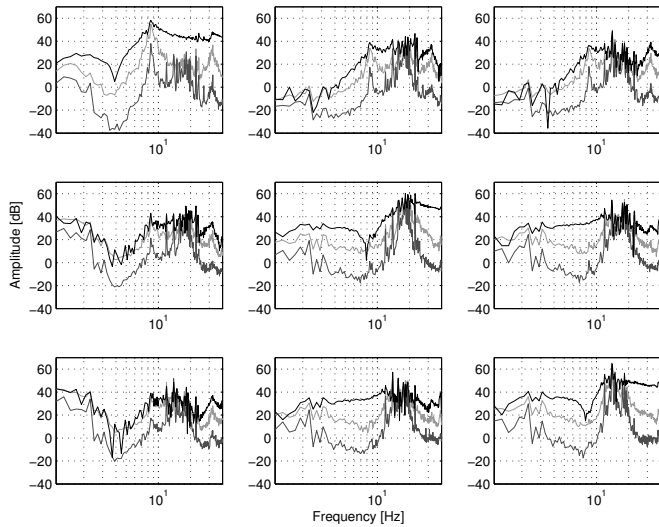


Fig. 7. Estimated FRF \hat{G} (black line) using data set 3. Grey line: standard deviation of the total sample variance $\hat{\sigma}_{\hat{G}}$. Dark grey line: standard deviation of the noise sample variance $\hat{\sigma}_{\hat{G}_n}$.

The estimation procedure according to (6) – (13) is then applied (taken element-wise) to the three different data sets. The estimated FRF, \hat{G} , can be seen in Figures 7 – 9 together with one standard deviation of the total sample variance $\hat{\sigma}_{\hat{G}}$ and the noise sample variance $\hat{\sigma}_{\hat{G}_n}$.

The influence of the excitation amplitude can be studied in Figures 7 and 8. As can be seen, a lower amplitude gives more fluctuations in the estimate, probably due to a lower SNR. For the (1,1) element one can also see a slightly increased anti-resonance frequency at 4 Hz, indicating a nonlinear stiffness.

Comparing Figures 8 and 9, one clearly sees the influence of static friction and the importance of using the square wave. In Figure 9, almost all resonances have disappeared for axis 2 and

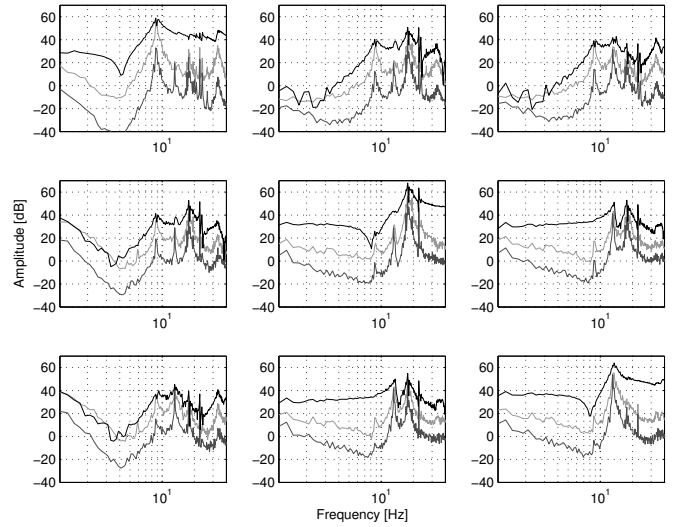


Fig. 8. Estimated FRF \hat{G} (black line) using data set 4. Grey line: standard deviation of the total sample variance $\hat{\sigma}_{\hat{G}}$. Dark grey line: standard deviation of the noise sample variance $\hat{\sigma}_{\hat{G}_n}$.

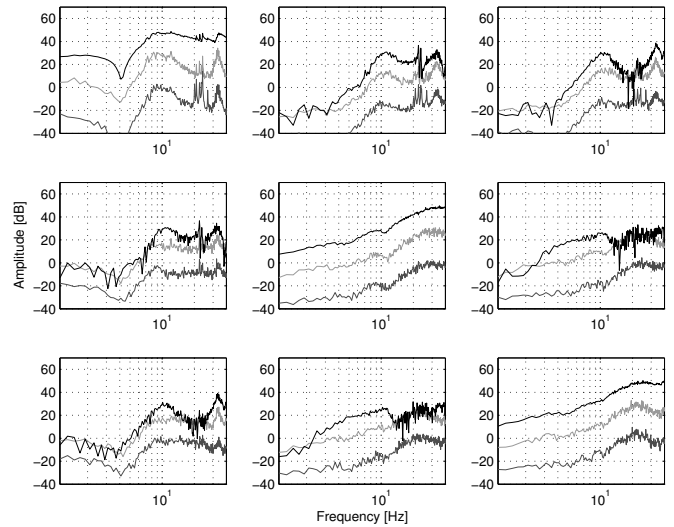


Fig. 9. Estimated FRF \hat{G} (black line) using data set 5. Grey line: standard deviation of the total sample variance $\hat{\sigma}_{\hat{G}}$. Dark grey line: standard deviation of the noise sample variance $\hat{\sigma}_{\hat{G}_n}$.

3. Still, similar to the SISO case, the variance of the estimate is increased around the resonance frequencies when using the square wave.

The FRF estimate in Figure 9 is, according to its sample variance, fairly accurate, but still almost all resonances have disappeared. How can this be the case? To answer this question, one should study the properties of $G_R(\omega_k)$ in (4), the best linear approximation to the nonlinear system. G_R could be considered as the sum of some “true” underlying linear system G_0 and a bias term G_B that depends on the excitation signal. Adding a square wave changes the shape of the excitation signal and will therefore change the bias term. The user must

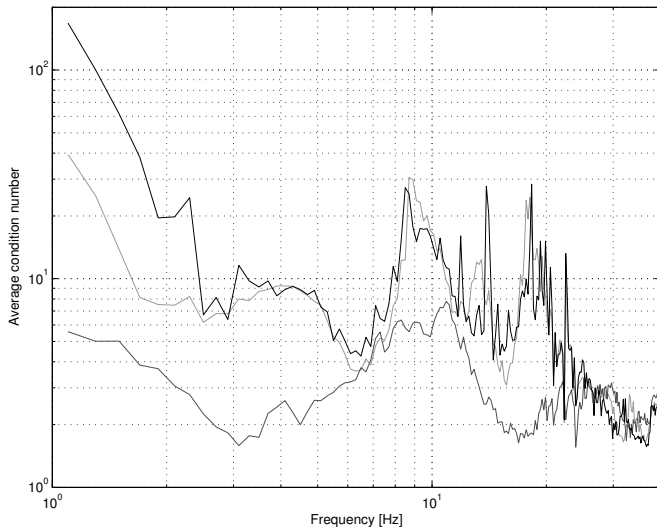


Fig. 10. Average condition number (over the $M = 9$ different blocks) of the input matrix for different data sets. Black line: data set 3, grey line: data set 4, dark grey line: data set 5.

therefore decide which “best” linear approximation that is most suitable for the modeling purpose and select a corresponding excitation signal for the experiments.

As was noted in the SISO case, the input SNR was a possible explanation for the increased variability in the estimates when using a square wave. For the MIMO case, it is required that the input matrix \mathbf{U} is invertible. The condition number of \mathbf{U} therefore gives valuable information. In Figure 10, the average condition number (over the $M = 9$ different blocks) of the input matrix can be seen for the three different data sets. As can be seen, the input matrix gets more ill-conditioned by adding the square wave. This is not only due to a reduced input power, but the square wave also increases the torque and resolver ripple (see [15], Chapter 8).

As was noted in [13], the MIMO FRF estimates tends to be non-symmetric, even if the underlying linear system is symmetric ($G_{kn} = G_{nk}$). This can be noted here as well for frequencies below 4 Hz, especially for the elements (1,2), (1,3), (2,1) and (3,1). These elements are also poorly estimated for low frequencies, indicated by having $|\hat{G}| \approx \hat{\sigma}_{\hat{G}}$.

V. CONCLUSIONS

A method for the detection and estimation of nonlinear distortions in an estimated FRF has successfully been applied to experimental data from an industrial robot. The results show that nonlinear distortions are indeed present and cause larger variability in the FRF than the measurement noise contributions. To get a more accurate FRF estimate one should therefore use available measurement time to average estimates from several experiments with random phase multisines. Averaging over several periods will not be as effective since that only reduces the measurement noise contributions.

Using a filtered square wave to reduce the effect of friction will give more pronounced resonances, but will at the same give larger variability in the FRF estimates due to a poorer SNR.

VI. ACKNOWLEDGEMENTS

This work has been supported by VINNOVA’s center of excellence ISIS at Linköpings universitet. The experiments have been carried out in the research lab of ABB Automation Technologies AB – Robotics, Västerås, Sweden, which is gratefully acknowledged. The authors also wishes to thank Johan Schoukens and Rik Pintelon for excellent guidance and many fruitful discussions.

- [1] K. Kozłowski, *Modelling and identification in robotics*, ser. Advances in Industrial Control. London: Springer, 1998.
- [2] F. Behi and D. Tesar, “Parametric identification for industrial manipulators using experimental modal analysis,” *IEEE Trans. Robot. Automat.*, vol. 7, no. 5, pp. 642–652, Oct 1991.
- [3] R. Johansson, A. Robertsson, K. Nilsson, and M. Verhaegen, “State-space system identification of robot manipulator dynamics,” *Mechatronics*, vol. 10, no. 3, pp. 403–418, Apr 2000.
- [4] A. Albu-Schäffer and G. Hirzinger, “Parameter identification and passivity based joint control for a 7DOF torque controlled light weight robot,” in *Proceedings of the 2001 IEEE International Conference on Robotics and Automation*, Seoul, Korea, May 2001, pp. 2852–2858.
- [5] E. Wernholt and S. Gunnarsson, “Nonlinear identification of a physically parameterized robot model,” in *IFAC System Identification Symposium SYSID 2006*, 2006.
- [6] R. Pintelon, G. Vandersteen, L. De Locht, Y. Rolain, and J. Schoukens, “Experimental characterization of operational amplifiers: A system identification approach – part I: Theory and simulations,” *IEEE Trans. Instrum. Meas.*, vol. 53, no. 3, pp. 854–862, Jun 2004.
- [7] R. Pintelon, Y. Rolain, G. Vandersteen, and J. Schoukens, “Experimental characterization of operational amplifiers: A system identification approach – part II: Calibrations and measurements,” *IEEE Trans. Instrum. Meas.*, vol. 53, no. 3, pp. 863–876, Jun 2004.
- [8] D. Hanselman, “Resolver signal requirements for high accuracy resolver-to-digital conversion,” *IEEE Trans. Ind. Electron.*, vol. 37, no. 6, pp. 556–561, Dec 1990.
- [9] H.-J. Gutt, F. D. Scholl, and J. Blattner, “High precision servo drives with DSP-based torque ripple reduction,” in *Proceedings of IEEE AFRICON, 1996*, vol. 2, Sep 1996, pp. 632–637.
- [10] R. Dhaouadi, F. H. Ghorbel, and P. S. Gandhi, “A new dynamic model of hysteresis in harmonic drives,” *IEEE Trans. Ind. Electron.*, vol. 50, no. 6, pp. 1165–1171, Dec 2003.
- [11] R. Pintelon and J. Schoukens, *System identification: a frequency domain approach*. New York: IEEE Press, 2001.
- [12] R. Pintelon and J. Schoukens, “Measurement of frequency response functions using periodic excitations, corrupted by correlated input/output errors,” *IEEE Trans. Instrum. Meas.*, vol. 50, no. 6, pp. 1753–1760, Dec 2001.
- [13] E. Wernholt and S. Gunnarsson, “On the use of a multivariable frequency response estimation method for closed loop identification,” in *Proc. of the 43rd IEEE Conference on Decision and Control*, Atlantis, Paradise Island, The Bahamas, Dec 2004.
- [14] T. Dobrowiecki and J. Schoukens, “Measuring linear approximation to weakly nonlinear MIMO systems,” in *Proc. 16th IFAC World Congress*, Prague, July 2005.
- [15] E. Wernholt, “On multivariable and nonlinear identification of industrial robots,” Department of Electrical Engineering, Linköping University, SE-581 83 Linköping, Sweden, Tech. Rep. Licentiate Thesis no. 1131, Dec 2004.

	Avdelning, Institution Division, Department Division of Automatic Control Department of Electrical Engineering	Datum Date 2006-08-29
	Språk Language <input type="checkbox"/> Svenska/Swedish <input checked="" type="checkbox"/> Engelska/English <input type="checkbox"/> _____	Rapporttyp Report category <input type="checkbox"/> Licentiatavhandling <input type="checkbox"/> Examensarbete <input type="checkbox"/> C-uppsats <input type="checkbox"/> D-uppsats <input checked="" type="checkbox"/> Övrig rapport <input type="checkbox"/> _____
URL för elektronisk version http://www.control.isy.liu.se		LiTH-ISY-R-2740
Titel Detection and Estimation of Nonlinear Distortions in Industrial Robots Title		
Författare Erik Wernholt, Svante Gunnarsson Author		
Sammanfattning Abstract System identification in robotics often involves the estimation of linear models characterizing the behavior in certain operating points. In this paper, a method for the detection and estimation of nonlinear distortions in an estimated frequency response function (FRF) has successfully been applied to experimental data from an industrial robot. The results show that nonlinear distortions are indeed present and cause larger variability in the FRF than the measurement noise contributions.		
Nyckelord Keywords Frequency response functions, multivariable systems, nonlinear distortions, non-parametric identification, industrial robots		